The earliest stars and their relics in the Milky Way

L. Gao[1,2⋆], Tom Theuns[2,3], C. S. Frenk[2], A. Jenkins[2], J. C. Helly[2], J. Navarro[4], V. Springel[5] and S. D. M. White[5]

[1] *National Astronomical Observationaries, Chinese Academy of Science, Beijing, 100012, China*
[2] *Institute of Computational Cosmology, Department of Physics, University of Durham,*
Science Laboratories, South Road, Durham DH1 3LE
[3] *Universiteit Antwerpen, Campus Groenenborger, Groenenborgerlaan 171, B-2020 Antwerpen, Belgium*
[4] *Department of Physics and Astronomy, University of Victoria, PO Box 3055 STN CSC, BC V8W 3P6, Canada*
[5] *Max-Planck Institute for Astrophysics, Karl-Schwarzschild Str. 1, D-85748, Garching, Germany*

14 January 2010

ABSTRACT

We have implemented a simple model to identify the likely sites of the first stars and galaxies in the high-resolution simulations of the formation of galactic dark matter halos of the *Aquarius Project*. The first star in a galaxy like the Milky Way formed around redshift $z = 35$; by $z = 10$, the young galaxy contained up to $\sim 3 \times 10^4$ dark matter haloes capable of forming stars by molecular hydrogen cooling. These minihaloes were strongly clustered and feedback may have severely limited the actual number of Population III stars that formed. By the present day, the remnants of the first stars would be strongly concentrated to the centre of the main halo. If a second generation of long-lived stars formed near the first (the first star relics), we would expect to find half of them within $30h^{-1}$kpc of the galactic centre and a significant fraction in satellites where they may be singled out by their anomalous metallicity patterns. The first halo in which gas could cool by atomic hydrogen line radiation formed at $z = 25$; by $z = 10$, the number of such 'first galaxies' had increased to ~ 300. Feedback might have decreased the number of first galaxies at the time they undergo significant star formation, but not the number that survive to the present because near neighbours merge. Half of all the "first galaxies" that form before $z = 10$ merge with the main halo before $z \sim 3$ and most lose a significant fraction of their mass. However, today there should still be more than 20 remnants orbiting within the central $\sim 30h^{-1}$kpc of the Milky Way. These satellites have circular velocities of a few kilometers per second or more, comparable to those of known Milky Way dwarfs. They are a promising hunting ground for the remnants of the earliest epoch of star formation.

Key words: methods: N-body simulations – methods: numerical –dark matter – galaxies: haloes – galaxies: structure, formation

1   INTRODUCTION

The first stars probably formed through molecular hydrogen cooling of gas compressed in dark matter potential wells (Couchman & Rees 1986; Tegmark et al. 1997; see Bromm & Larson 2004 for a recent review). The temperature of the gas needs to be $\geq 10^3$K for H_2 formation to be efficient; in a ΛCDM universe dark matter haloes with deep enough potential wells to heat the gas to this temperature form as early as redshift $z \sim 50$ (Gao et al. 2004, Reed et al. 2005).

Such stars were very massive, $M \sim 10^2\,M_\odot$ (Abel, Bryan & Norman 2000; Bromm, Coppi & Larson 2002; Yoshida et al. 2007; Gao et al. 2007) and, depending on their initial mass, would have ended their short lives as supernovae or by collapsing directly into a black hole (Heger et al. 2003). In neither case can the remnants be identified today.

Very massive first stars ('Population III' or 'Pop. III' stars) emit copious amounts of UV photons (Schaerer 2002) which may affect star formation in nearby haloes through photoevaporation (Shapiro, Iliev & Raga 2004; Whalen et al. 2008) and/or destruction of molecular hydrogen by photons in the Lyman-Werner bands (Haiman, Rees

⋆ Email:lgao@bao.ac.cn

& Loeb 1997). These photons could contribute to the reionization of the Universe (e.g. Sokasian et al. 2004). Elements synthesised during stellar evolution may pollute the surroundings, affecting the cooling rate of gas (Bromm, Yoshida & Hernquist 2003). The combined 'feedback' of photoionisation, energy injection and changes in composition may allow the formation of lower mass stars ($M \sim 40 M_\odot$, Yoshida et al. 2007) and their feedback may eventually allow the formation of even lower mass stars, some of which could still be present today. These very old stars could provide 'archaeological' evidence for early star formation through, for example, unusual element abundance patterns (*e.g.* Iwamoto et al. 2005). As structure formation progresses, more massive dark matter haloes form in which gas can now cool by radiation from *atomic* hydrogen. This can occur as early as redshift $z \sim 40$ (Reed et al. 2005). Star formation in such 'first galaxies' may be very different from that in the first haloes (see e.g. Wise & Abel 2008) because of more efficient cooling by HI and the metals released by previous Pop. III stars.

There are currently no direct observational constraints on this scenario and so many uncertainties remain. For example, first star formation in a Universe where structure on small-scales is suppressed due to free-streaming of the dark matter (as in Warm Dark Matter models) is very different (Gao & Theuns 2007); annihilating dark matter, not fusion, may power the first stars if the dark matter consists of Majorana particles (Freese et al. 2008). Whilst the initial stages of cloud collapse can be understood in terms of the properties of the H_2 molecule (Abel et al. 2002; Yoshida et al. 2006), uncertainties from the modelling of radiative feedback of the proto-star make the final stellar mass uncertain (McKee & Tam 2008), although the general view is that these stars are massive. The second generation stars may, in fact, have relatively high metallicity if metal mixing is inefficient. Ionisation front instabilities (Whalen and Norman 2008) and the explosive growth of H_2 following photoionization may also strongly affect the next generation of stars (Whalen et al. 2008).

A number of important questions remain unanswered. Did star formation in the Milky Way galaxy start with a display of fireworks? If so, where should we look for archaeological evidence? Will most very old stars be in the bulge (White & Springel 2000) or will some be found in the halo? Two recently discovered 'hyper metal poor' stars ([Fe/H] < -5) have peculiar element abundances. Were these second-generation stars enriched by the first stars[1] (see the review by Beers & Christlieb 2005)? Finding more such unusual stars in the Milky Way is a key science driver for new surveys such as SEGUE, and LAMOST. Did any of the first galaxies survive to the present day? Where are their remnants? Are they related to the newly discovered dwarfs (Willman et al. 2005; Belokurov et al. 2006), as discussed in a number of recent papers (Madau, Diemand & Kuhlen 2008; Bovill & Ricotti 2009; Koposov et al. 2009). If so, what constraints do these place on the

earliest star formation? Helmi et al. (2006) argued that the remnants of early star formation in the Milky Way differ from those in dwarf galaxies because the latter had already been polluted with metals. However, Kirby et al. (2008) drew the opposite conclusion from more detailed modelling of stellar metallicities.

In this paper we address some of these questions using a suite of ultra-high resolution cosmological dark matter simulations of galactic haloes – the *Aquarius Project*. The six dark matter haloes data from the *Aquarius Project* picked from a large cosmological simulation to be similar in mass to that of the Milky Way, and they were simulated at a variety of numerical resolutions. This enables us to investigate halo-to-halo variations, and establish the limitations imposed by resolution. We employ simple models to identify the sites of first star or first galaxy formation and follow a suitable selection of dark matter particles to track where their progenitors are today, yielding generic cold dark matter predictions for early star formation in galaxies like the Milky Way.

The outline of the paper is as follows. In Sections 2, 3 and 4 respectively we describe the simulations, our models for identifying first star and first galaxy haloes, and investigate the clustering of these haloes. In Section 5 we trace the early objects to $z = 0$ and discuss their properties and spatial distribution. Finally, in Section 6 we present a summary and discussion of our results.

2 SIMULATIONS

The dark matter simulations analyzed in this study come from the *Aquarius Project*[2] (Springel et al. 2008a, b; Navarro et al. 2009): a set of six haloes similar to that of the Milky Way (virial mass $M_{200} \sim 10^{12} h^{-1} M_\odot$, circular velocity $V_{200} \sim 180$ km s^{-1}, where the subcript 200 refers to the region within which the density is 200 times the cosmic critical density; see Table 1). The halos were identified in a larger cosmological simulation, the hMS simulation (Gao et al. 2008), which follows the growth of structure in a periodic box of comoving length $100 h^{-1}$Mpc with 900^3 particles, assuming the same cosmological parameters as in the Millennium simulation[3] (Springel et al. 2005): $\Omega_m = 0.25, \Omega_\Lambda = 0.75, h = 0.73, \sigma_8 = 0.9$. The hMS is itself a lower resolution version of the Millennium-II simulations[4] (Boylan-Kolchin et al. 2009), so that the *Aquarius* haloes are alos present in the Millennium-II simulation.

Resimulating the formation of haloes in such a large box correctly accounts for tidal forces and yields realistic formation times. The 'zoom' technique for resimulating haloes represents the mass which ends up inside or near the chosen halo with many low mass particles and a small gravitational softening; the mass in more distant regions is represented with increasingly more massive particles with larger gravitational softening. Appropriate small-scale power is added in the initial conditions to perturb the

---

[1] We will refer to nearly primordial stars contaminated only by metals from the first stars as 'first star relics'.

high-resolution particles. The haloes, labelled Aq-A to Aq-F, are simulated with up to 10^9 particles within the virial radius (particle mass $\sim 10^{3-4}h^{-1}M_\odot$), using the Gadget-3 simulation code which is an updated version of Gadget-2 (Springel 2005). The Aq-A halo has been resimulated at different resolutions in order to study numerical convergence.

Snapshots are stored at 128 output times equally spaced in $\log(a)$, where $a = 1/(1+z)$ is the expansion factor, between redshifts $z = 127$ and $z = 0$. Dark matter haloes and their substructure are identified using a combination of the friends-of-friends algorithm (Davis et al. 1985) and SUBFIND (Springel et al. 2001). SUBFIND groups particles into substructures based on their density and binding energy. Haloes and their substructure are traced through the snapshots and linked together in a merger tree, as in Cole et al. (2008).

Although the *Aquarius* haloes range in mass only from $0.6 \times 10^{12}h^{-1}M_\odot$ to $1.3 \times 10^{12}h^{-1}M_\odot$, their mass accretion histories, plotted in Fig. 1, differ significantly. For example, the mass of the main progenitor of the Aq-F halo is nearly an order of magnitude lower than that of Aq-C as late as $z \sim 1$, and similarly large differences occur for other haloes at higher z. The thick dashed line is the extended Press-Schechter (Press & Schechter 1974; Bond et al. 1991; Lacey & Cole 1993) prediction for a halo of the median mass, $M = 1.3 \times 10^{12}h^{-1}M_\odot$, computed following Gao et al. (2004a). Apart from a systematic overestimate of the mass at high redshift ($z > 20$), the prediction works well.

3   IDENTIFYING SITES OF HIGH-REDSHIFT STAR FORMATION

In this section, we describe a simple model for identifying those haloes in the simulations which are likely to be the sites of early star formation.

3.1   Sites of Pop. III star formation

Our model is based on the results of a suite of hydrodynamical simulations of the formation of early structures in a ΛCDM cosmology, carried out by Gao et al. (2007), which included nine-species, non-equilibrium gas-phase chemistry of H_2 production. The simulations used zoomed initial condition to follow the collapse to high densities ($n_H \sim 10^{10}\mathrm{cm}^{-3}$) of gas in haloes with a wide range of formation redshifts ($50 > z > 10$) and masses ($10^5 h^{-1}M_\odot < M <$ a few $\times$ $10^6 h^{-1}M_\odot$), and investigated how this depends on the assumed cosmological parameters. In agreement with previous studies (e.g. Abel et al. 2002; Bromm et al. 2002; Yoshida et al. 2006), these authors found that the virial temperature, $T_{\rm vir}$, of the parent dark matter halo is the key physical parameter that regulates how efficiently gas collapses and cools.

Once $T_{\rm vir} \geq 10^3$ K, the formation of molecular hydrogen becomes very efficient, a significant molecular hydrogen abundance ($f_{H_2} \sim 10^{-4}$) builds up and the gas cools rapidly, becomes self-gravitating and collapses to higher and higher densities, presumably culminating in the formation of a
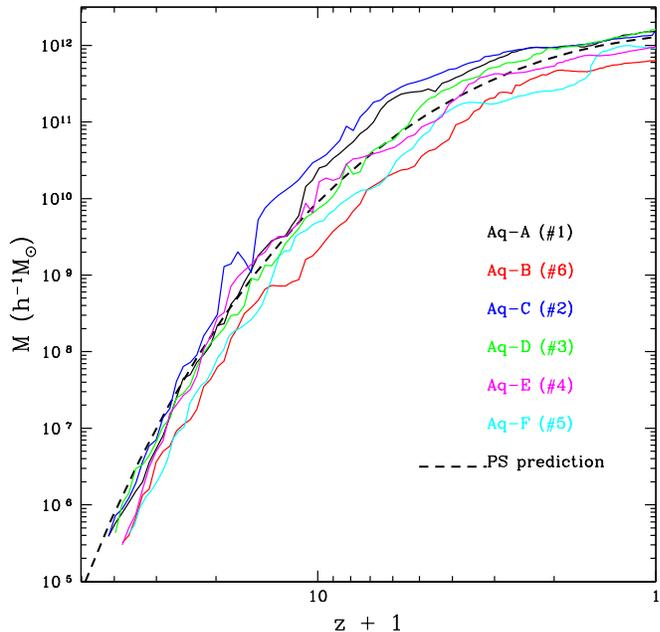
Figure 1. Mass of the most massive progenitor of each of the six *Aquarius* haloes as a function of redshift ($M(z)$, coloured lines), compared to the extended Press-Schechter (ePS) theory for a halo of mass equal to the median for the six halos, $M = 1.3 \times 10^{12}h^{-1}M_\odot$ (dashed line). There is over an order of magnitude variation in $M(z)$ between the haloes at certain redshifts, even though the $z = 0$ masses are all within a factor of two (The number in brackets sorts haloes by their $z = 0$ mass.). The ePS prediction works well, but systematically overestimates the mass above $z \sim 20$.

star. The duration of this process scales with the dynamical time of the halo and is typically $\Delta z \sim 3 - 4$; during this time, a halo may increase its mass significantly through mergers and accretions. Therefore neither the instantaneous halo mass, nor the virial temperature, are sufficient to describe the star forming properties of a halo; its merger history needs to be taken into account.

Gao et al. (2007) developed a simple model of Pop. III star formation, based on the merger trees of the parent halos, which quite accurately matches the Pop. III star formation properties of all 8 individual objects simulated in that study. Define the virial temperature $T_{\rm vir}$ of a halo in terms of its circular velocity, V_{200}, at a radius R_{200} (within which the mean density equals 200 times the critical density) as

$$k_{\rm B}\,T_{\rm vir} \equiv \frac{1}{2}\,\mu\,m_{\rm p}\,V_{200}^2\,, \tag{1}$$

where $k_{\rm B}$ is Boltzmann's constant, μ is the mean molecular weight ($\mu = 1.22$ for neutral H-He admixture), and $m_{\rm p}$ is the hydrogen mass (e.g. White & Frenk 1991). Once the virial temperature reaches $T_{\rm min} = 1100$ K (or, equivalently, the circular velocity exceeds $V_{200,\rm min} = 4\mathrm{km\,s}^{-1}$), a star is assumed to form after a redshift delay of $\Delta z \sim 3 - 4$. We

Name	$m_{\rm p}[h^{-1}{\rm M}_\odot]$	$\epsilon[h^{-1}{\rm pc}]$	$M_{200}[h^{-1}{\rm M}_\odot]$	$r_{200}[h^{-1}{\rm kpc}]$	$V_{\rm max}[{\rm s}^{-1}{\rm km}]$	$V_{200}[{\rm s}^{-1}{\rm km}]$
Aq-A-1	1.25×10^3	15.0	1.34×10^{12}	179.40	208.8	179.2
Aq-A-2	1.00×10^4	48.0	1.34×10^{12}	179.40	208.5	179.2
Aq-B-2	4.70×10^3	48.0	0.60×10^{12}	136.51	157.7	137.5
Aq-C-2	1.02×10^4	48.0	1.30×10^{12}	177.26	222.4	177.6
Aq-D-2	1.02×10^4	48.0	1.30×10^{12}	177.26	203.2	177.6
Aq-E-2	7.00×10^3	48.0	0.87×10^{12}	155.00	179.0	155.4
Aq-F-2	4.95×10^3	48.0	0.83×10^{12}	152.72	169.1	153.2

Table 1. Properties of the six *Aquarius* haloes, Aq-A – Aq-F. The Aq-A halo has been resimulated at a variety of numerical resolutions, labelled Aq-A-1 – Aq-A-5. (In this paper, we analyze only Aq-A-1 and Aq-A-2.) From left to right the columns give: the halo identifier, particle mass, (comoving) force softening length in the high-resolution region, virial mass, virial radius, and maximum and virial circular velocity, all at redshift $z = 0$ (M_{200}, r_{200}, $V_{\rm max}$ and V_{200}, respectively).

apply this model to identify which haloes form Pop. III stars, and when.

The first star may suppress or enhance star formation in neighbouring halos through the combined effect of its ionising and Lyman-Werner radiation (e.g. Haaiman, Rees & Loeb 1996; Machacek et al. 2003; Yoshida et al. 2003, Wise & Abel 2008; Whalen et al. 2008). The net effect is still unclear and so we introduce below a simplified feedback model based on the spatial clustering of the haloes.

3.2   Sites of the first galaxies

Once the virial temperature of the halo is high enough for atomic line cooling of gas to become important, $T_{\rm vir} \sim 6000$ K, we assume that the nature of star formation changes. Rather than a single, massive primordial star per halo, the cooling of the metal-enriched gas is assumed to lead to the formation of a normal stellar population with a range of masses. The depth of the potential well of these 'first galaxy' haloes is still so shallow that even a single supernova explosion can produce strong winds, as in the classic White & Rees (1978) picture, leading to bursty behaviour which is difficult to model; see e.g. Mori, Ferrara & Madau (2002); Yoshida et al. (2007); Wise & Abel (2008); Greif et al. (2008); Bromm et al. (2009). Whether it is simply the contribution of atomic lines to cooling that leads to the formation of lower mass stars alongside massive ones, or that of metals or dust (Schneider et al 2006), or the change in the turbulent properties of the star-forming gas (Krumholtz & McKee 2005), or all of the above, is presently unclear. Given these uncertainties, we adopt the simple criterion, $T_{\rm vir} \geq 10^4$ K, to separate haloes that form Pop. III stars from 'first galaxy' halos that form stars with a broader IMF. Of course, if feedback from one halo strongly affects star formation in its surroundings, this distinction may be too simplistic.

4   FORMATION HISTORY AND CLUSTERING OF STAR FORMING HALOES

The general picture of early star formation sketched above changes dramatically as soon as the star-forming gas becomes ionised, either through photons emitted by nearby stars, or because the universe as a whole becomes ionised. The photo-heating of the gas and the suppression of atomic cooling quenches star formation in dwarf galaxies with circular velocity, $V_{\rm max} \leq 25$ km s^{-1} (e.g. Efstathiou 1992; Thoul & Weinberg 1996; Gnedin 2000; Hoeft et al. 2006; Okamoto, Gao & Theuns 2008). The Thomson scattering optical depth towards the last scattering surface, as determined from the WMAP data (Komatsu et al. 2008), suggests that the universe was reionized at a redshift, $z_r \sim 10$. We will consider earlier times, $z > z_r$, when the Universe was still mainly neutral, and star formation could take place in haloes with circular velocity as small as a few kilometers per second.

4.1   The first stars in galaxies like the Milky Way

Figure 2 shows the evolution in the number of *Aquarius* progenitor dark matter haloes that, in the absence of feedback, would be able to form Pop. III stars. The numbers are calculated either using a simple virial temperature criterion (full lines) or the more detailed model of Gao et al. (2007; dashed lines). Star formation begins around $z \sim 40$ ($z \sim 35$ in the Gao et al. 2007 model), and the number of star-forming progenitor haloes increases very rapidly to reach 10^3 at $z \sim 30$ and 10^4 at $z \sim 15$; thereafter the numbers decrease as the haloes begin to merge. The halo-to-halo variation remains relatively small up to $z \sim 20$ but, by $z \sim 10$, it has increased to about a factor of five, with more massive *Aquarius* haloes tending to have more star forming progenitors at $z \sim 10$.

The difference in the number of star-forming haloes predicted by the simple, $T_{\rm vir} = 1100$ K, cut and the Gao et al. (2007) model is large, of order a factor 10 or more at $z \geq 15$. The reason for this difference is the delay (by $\Delta z \approx 3$) in the onset of star formation in the Gao et al. model at a time when the number of star-forming objects is rising extremely rapidly. Once the number of star-forming haloes reaches its maximum, the two models agree to
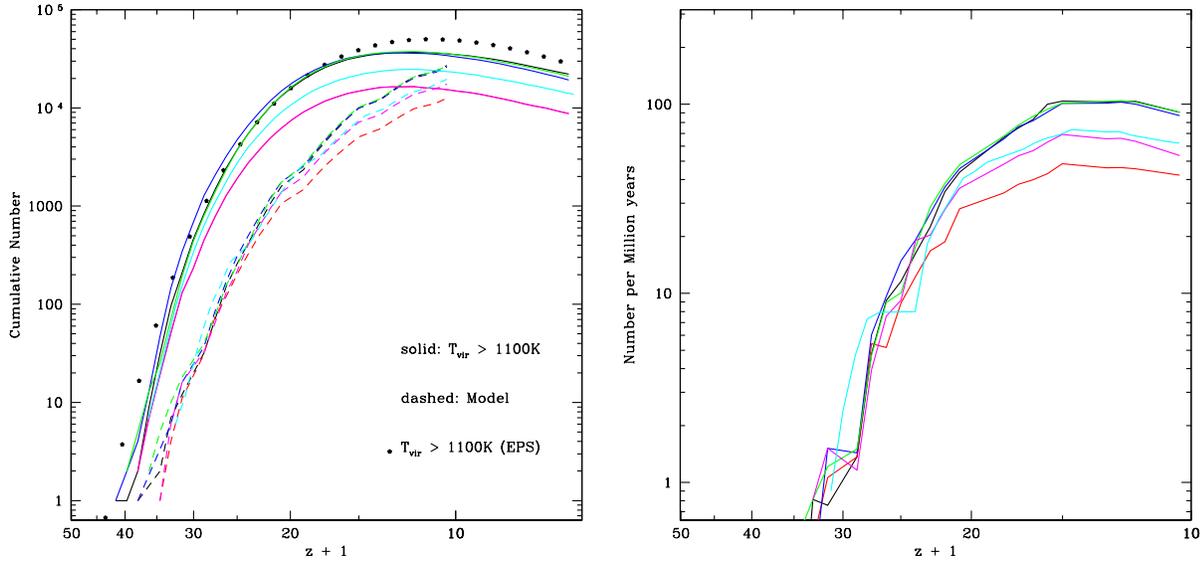
Figure 2. Pop. III star formation in galaxy halo progenitors as a function of redshift. *Left panel*: cumulative number of progenitor haloes with virial temperature above 1100 K for each of the six *Aquarius* haloes (colour solid lines). The black dots show the extended Press-Schechter prediction which works well, but increasingly overestimates the number of halos after $z \sim 15$. Gas in such haloes is hot enough for significant H_2 formation. The dashed lines show the cumulative number of independent sites of Pop. III star formation according to the model of Gao et al. (2007) which, in addition to a virial temperature criterion, takes the merger history of the halo into account. This more stringent criterion reduces the number of forming stars; yet a Milky Way-type halo still had several hundreds of Pop. III star-forming progenitors at redshift $z = 25$ and $\sim 10^4$ at $z = 10$. The halo-to-halo variation is large, a factor ~ 5 at $z = 10$. The cumulative number of haloes drops after $z \sim 10$ as haloes begin to merge. *Right panel*: the star formation rate. The rate increases from a few star forming events per Myr at $z = 30$, to several tens at $z = 20$ and changes little thereafter.
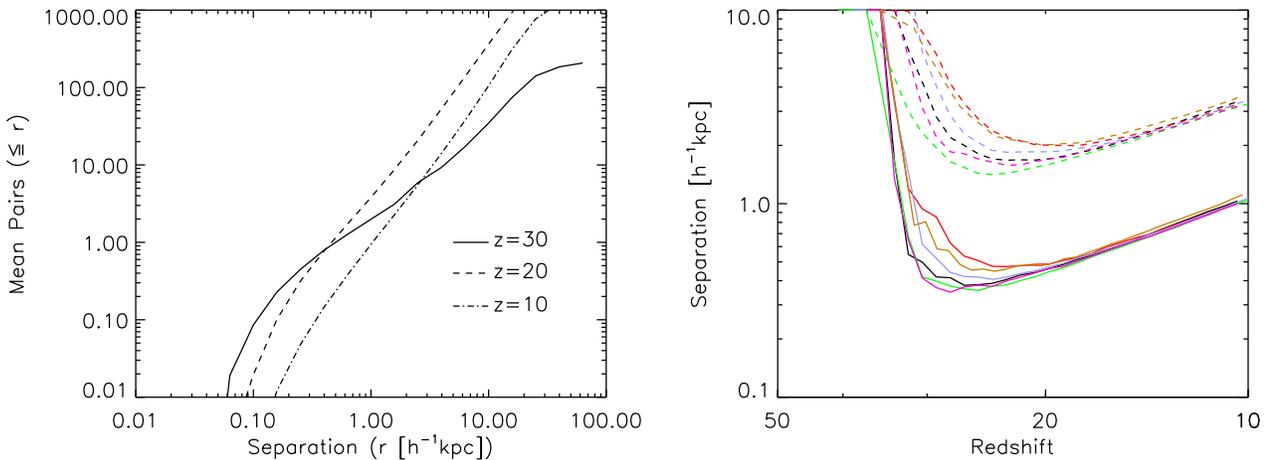
Figure 3. Clustering of Pop. III star-forming progenitor haloes. *Left panel:* mean number of progenitor halo pairs in Aq-A, as a function of proper separation at the three redshifts indicated in the panel. *Right panel*: mean separation of progenitor haloes in each of the six *Aquarius* haloes. Each halo has one neighbour within the distance given by the solid line, and 10 neighbours within the distance given by the dashed lines. Star-forming halos have relatively nearby companions, indicating that feedback effects could be important (see text). The linear rise in separation between substructures below $z \sim 20$ is because the proto-halo region is still expanding with the Hubble flow at this early time.

within a factor of a few. The star formation rate is of order $\dot{N}_\star \approx 1\,\mathrm{Myr}^{-1}$ at $z = 30$, increasing rapidly to reach a broad peak of $\dot{N}_\star \approx 10^2\,\mathrm{Myr}^{-1}$ at $z \sim 15$. According to the Gao et al. model, the first stars in a Milky Way sized halo appear around $z \sim 35$, later than in a proto-cluster where star formation starts around $z \sim 47$ (Gao et al. 2007).

So far we have neglected potential feedback effects, arising from star formation, on neighbouring haloes which could, in fact, be quite severe. UV photons with energy, $h\nu > 13.6$ eV, emitted by massive stars may ionise and heat the gas in a neighbouring halo. Star formation may thus be quenched due to the suppression of atomic cooling and photo-heating, or altogether prevented as the halo loses gas through photo-evaporation (e.g. Shapiro, Iliev & Raga 2004; Whalen et al. 2008, Okamoto et al. 2009). On the other hand, H_2 formation may be enhanced in photo-ionised gas, once the source of ionising photons has faded (Haiman, Rees & Loeb 1996). These effects will be mostly restricted to the HII region surrounding the star because of the high optical depth of ionising radiation, except for the high-energy tail of the photon energy distribution.

Lyman-Werner photons with $11.2 \leq h\nu/\mathrm{eV} \leq 13.6$ may destroy the H_2 coolant, also quenching or suppressing star formation. Most of the gas is optically thin to Lyman-Werner photons and so this 'sphere of influence' extends beyond the edge of the HII region. However, some star-forming haloes may become dense enough to self-shield, even in the Lyman-Werner bands. Kinematical feedback from the star in the form of a stellar wind or supernova explosion, may also affect its surroundings.

Clearly, the details of these feedback effects are difficult to model accurately, and so the degree of suppression of star formation near a Pop. III star remains highly uncertain (see Yoshida et al. 2003; O'Shea & Norman 2007 and 2008; Wise & Abel 2008; Yoshida et al. 2008; Whalen et al. 2008; Ahn & Shaprio 2006, for recent discussions). In view of this, we have developed a simple model for feedback that takes into account the clustering of the halos. We consider only radiative feedback and neglect external radiation from distant stars or galaxies. For each progenitor halo, we calculate the average number, $N(r)$, of neighbouring potentially star-forming haloes a function of separation, r. The number of neighbours, shown in Fig. 3, scales roughly as $N(r) \sim r^2$. At $z = 30$, the typical pair separation is $r \sim 1 h^{-1}\mathrm{kpc}$(note that here and below we give seperations in proper, not comoving units).

A more direct measure of the redshift evolution of clustering is the mean separation of pairs, $N(1)$, and the mean distance to the 10th star-forming nearest neighbour halo, $N(9)$, as a function of redshift, also shown in Fig. 3. Both curves fall rapidly with decreasing redshift as haloes begin to form in profusion, reach a minimum between $z = 30 - 20$ and thereafter increasing slowly due to Hubble expansion of the proto-galactic region. On average, each potentially star-forming halo has another potentially star-forming halo within $0.5 h^{-1}\mathrm{kpc}$ at $z = 30$, increasing slowly to $0.6 h^{-1}\mathrm{kpc}$ at $z = 20$, and ten others within $2 h^{-1}\mathrm{kpc}$ over the same redshift range.

To estimate the effect of feedback from ionising radiation, we compare these numbers to the radius, R, of an HII region in a uniform density medium,
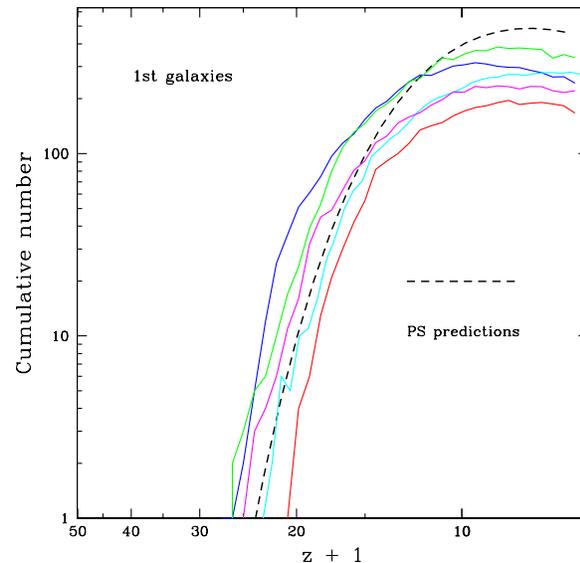

Figure 4. The abundance of haloes hosting 'first galaxies' (virial temperature $T_{\mathrm{vir}} > 10^4$ K) as a function of redshift for the six *Aquarius* haloes (colours are the same as in Fig. 1). Dashed lines are the prediction from extended Press-Schechter theory. These haloes start to appear around $z \sim 25$ and their abundance rises rapidly to reach a broad peak of 200-300 haloes by $z \sim 10$. Progenitors of haloes more massive at $z = 0$ tend to have a higher abundance of first galaxy haloes at all z.

$$R = 1.3 \left(\frac{\dot{N}_\gamma}{10^{50}\,\mathrm{s}^{-1}} \frac{\Delta t}{3\mathrm{Myr}} \frac{100}{1+\delta} \right)^{1/3} \frac{10}{1+z}\,\mathrm{kpc}\,, \qquad (2)$$

around a source emitting ionising photons at a rate, $\dot{N}_\gamma$, over a time interval, Δt. The medium is at an overdensity, δ, has the cosmological baryon fraction, $\Omega_b h^2 = 0.045$, and a hydrogen abundance of 0.75 by mass. Full numerical simulations find similar radii for the HII region (e.g. Abel et al. 2007, Yoshida et al. 2007). The fact that R is comparable to the mean interhalo separation implies that feedback from ionising photons could indeed be rather important in quenching first star formation. The formation rate of first stars could then be significantly smaller than the no-feedback case depicted in Fig. 2.

4.2   The first galaxy haloes

Progenitors of *Aquarius* haloes first achieve a virial temperature, $T_{\mathrm{vir}} > 10^4$ K, around $z \sim 25$; the abundance of such "first galaxy" halos rises rapidly to a few tens by $z \sim 18$ and reaches a broad peak of ~ 300 by $z = 10$, as shown in Fig. 4. The scatter amongst the six *Aquarius* haloes is large. The rise in abundance is reasonably well described by the Press-Schechter formula, but this overestimates the number at $z = 10$ by ~ 50 percent. As was the case for Pop. III haloes discussed earlier, the first galaxy haloes in a proto-Milky Way object form at $z \sim 25$, substantially later than in a proto-cluster region where they form at $z \sim 40$ (Gao et al. 2004a). The more massive $z = 0$ *Aquarius* haloes
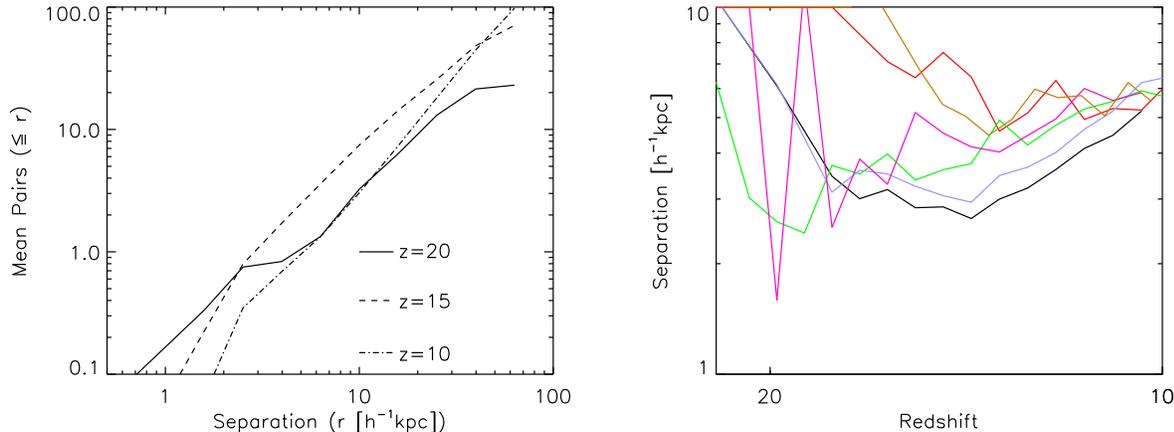
Figure 5. Clustering of 'first galaxy' progenitor haloes (virial temperature, $T_{\rm vir} > 10^4$ K). *Left Panel*: mean number of progenitor halo pairs in Aq-A, as a function of proper separation, at the redshifts indicated in the panel. *Right Panel:* redshift evolution of the mean separation between pairs of haloes with $T_{\rm vir} > 10^4$ K. By $z = 10$, the mean separation between first galaxy haloes is $\sim 6\ h^{-1}$kpc and each halo has on average another 10 haloes within $\sim 20\ h^{-1}$kpc. The typical distance to a neighbouring halo has a large scatter amongst realizations, reflecting the fact that these haloes only just began to form at these early times.

tend to have more first galaxy progenitors at $z \sim 10$.

As before, we characterise the clustering of haloes that can cool through atomic processes by the number of neighbours, $N(r)$, at distance r. As shown in Fig. 5, $N(r)$ is again approximately a power-law, $N(r) \propto r^2$. At $z = 10$, a first galaxy halo has a neighbouring first galaxy halo within $\sim 6\ h^{-1}$kpc and ~ 10 within $\sim 25\ h^{-1}$kpc. The halo-to-halo scatter in clustering properties is large at early redshift $z \sim 20$ (Fig. 5, right panel), but as more haloes form, it decreases; the typical separation reaches $r \sim 6\ h^{-1}$kpc at $z = 10$. Consequently, the ionised regions formed by star formation around such first galaxies need not be very large, of order a few h^{-1}kpc before HII regions percolate across a proto-Milky Way galaxy by $z = 10$.

Feedback from star formation in a first galaxy may potentially affect a neighbouring halo. Figure 6 displays the fraction of halos that would be affected depending on the value of the radius, R, of influence of the feedback, when taking clustering into account. For $R = 1h^{-1}$kpc, feedback has no effect, but for $R = 5\ h^{-1}$kpc, 20-30 percent of potential first galaxy halos could be affected, rising to 40-50 percent for $R = 10h^{-1}$kpc.

5 RELICS OF EARLY STAR FORMATION

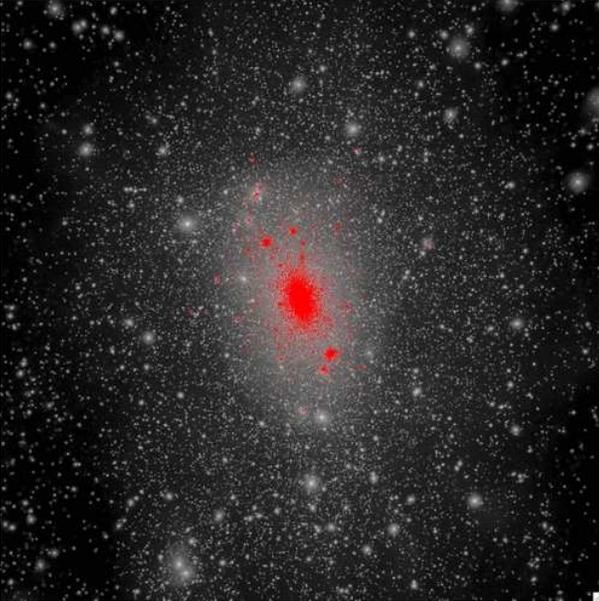## 5.1 Relics of the first stars

If, as seems likely, the first stars that form in a CDM universe are massive, then only their dark remnants will remain in the Milky Way today. However, evidence for their existence may be hidden in the anomalous abundance patterns of long-lived second generation stars that formed nearby, in gas predominantly enriched by Pop. III stars (e.g. Beers & Christlieb 2005; Rollinde et al 2008); we will call such stars 'first star relics '. Where are these fossils of primordial star formation to be found today? To answer this question, we
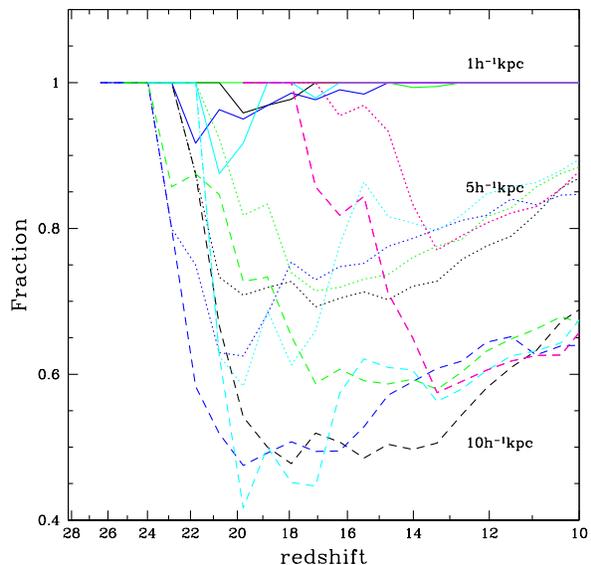

Figure 6. Fraction of first galaxies *not* affected by neighbouring first galaxies as a function of redshift, if the radius of influence of the feedback is R =10, 5 or 1 h^{-1}kpc (dashed, dotted, and solid lines, respectively). For the smaller value of R, feedback has little or no effect, but for larger R, feedback may decrease the number of first galaxies considerably, up to a factor ~ 2.

make use of the merger history of the haloes hosting primordial stars which is readily available in the simulations.

It seems reasonable to assume that feedback from Pop. III stars will have prevented the gas enriched by them from forming further stars until it is accreted later into a first galaxy halo where it can cool by atomic processes (see e.g. the simulations of Wise & Abel 2008). The earliest generation of stars formed in such a first galaxy may then have

Figure 7. Projected distribution at $z = 0$ of first star relics (red), compared to that of the dark matter for the Aq-A-2 halo. A significant fraction of the stars lie in the central part of the main galaxy, but some end up in dark matter subhalos. The image is 1080 kpc on a side, approximately twice the diameter of the virialised dark matter halo.
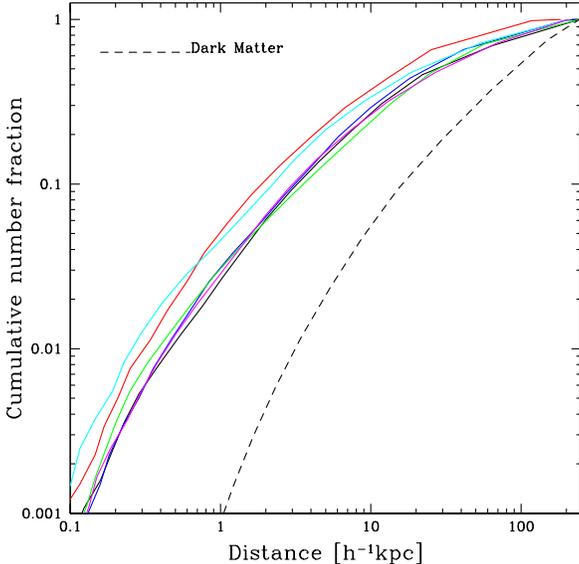
Figure 8. Cumulative distribution of second generation, first star relics, stars at redshift $z = 0$ for all six *Aquarius* haloes (colour lines), compared to the dark matter profile for the Aq-A halo (dashed black line).

the peculiar abundance pattern characteristic of Pop. III nucleosynthesis. However stars that form later may have been enriched by the elements produced by the previous generation of relatively metal rich stars, so that eventually the net abundance pattern loses its characteristic Pop. III star signature. To implement this idea we proceed as follows. We assume that each first galaxy halo contains a fixed *total mass* of **'first star relics'** - **stars that form in an environment enriched solely by truly primordial stars** – independent of redshift. To trace the location of such stars at later times, we tag the $N = 100$ most bound particles **at the time the virial temperature of the halo first exceeds** $T = 10^4$ **K** [5]. This assumes that these second-generation stars form in the centres of such dark-matter haloes. Once a halo has started forming stars, it will grow in mass, and may merge with other haloes. The number of first star relics in a halo will only change if it merges with a halo that contains its own population of first star relic stars. We continue tagging first star relics in haloes that reach the threshold T_{vir} until $z = 10$, after which we assume that reionisation of the Universe evaporates all mini-haloes.

In summary, we identify the epoch when a halo is first capable of sustaining gas that can cool through atomic processes and tag its 100 most bound particles as the first star relics, until $z = 10$. We can then investigate the spatial distribution of these first star fossils at any later epoch by tracing the tagged particles. The location of the first star relics today is illustrated in Fig. 7 where, for clarity, we show only a fraction of the stars. The image shows that most of the first star relics end up in the central regions of the halo, but some survive inside subhalos.

The visual impression gained from Fig. 7 is quantified in Fig. 8 which shows that the distribution of the first star relics today (which is similar in all six *Aquarius* halos) is expected to be much more concentrated than that of the dark matter. Fifty percent of these first star relics lie within $20h^{-1}$kpc of the centre and ~ 10 per cent lie inside what would be the galactic bulge, at $r < 2h^{-1}$kpc. In contrast, only ~ 10 percent of the dark matter lies within $20h^{-1}$kpc, and only about 0.1 percent is at $r < 1h^{-1}$kpc. Even though the stars in our simulations are already very concentrated, earlier models of the remnants of PoP-III stars (White & Springel 2000; Diemand et al. 2005) suggested they should be even more concentrated, with almost all of them lying in the bulge where they would be very hard to detect.

Although most of the first star relics reside in the central parts of the main halo, a significant fraction end up in dark matter subhalos. This is interesting because it may be easier to detect such unusual stars in a nearby dwarf galaxy than to hunt for them in the crowded surroundings of the Milky Way bulge.

5.2   Relics of the first galaxies

In this section we investigate the fate of first galaxy halos. As discussed in Section 4.2, these are dark matter halos which formed before $z = 10$ and have $T_{vir} > 10^4$ K. We are particularly interested in descendants which today are to be found

---

[5] We verified that our final results do not depend strongly on the arbitrary choice of N.
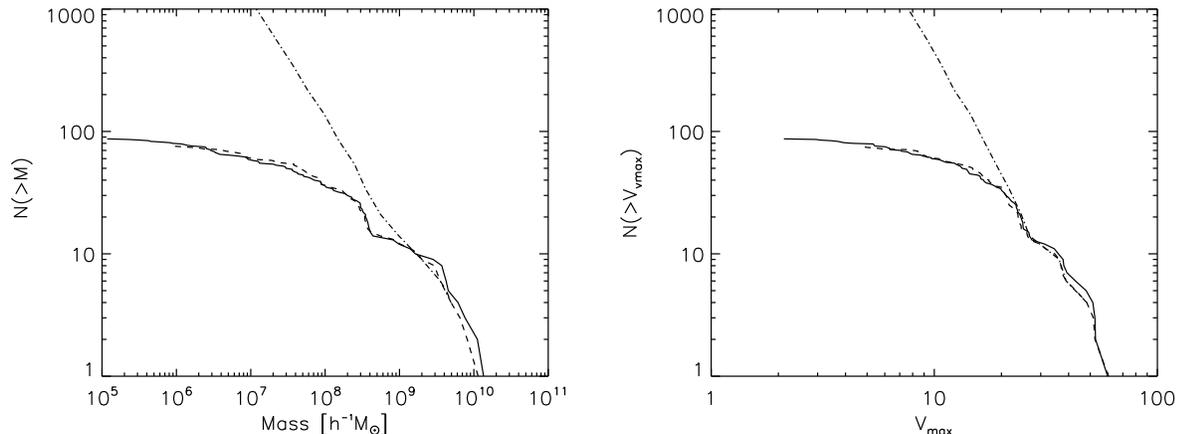
Figure 9. *Left panel*: Cumulative mass function at $z = 0$ of 'first galaxy' haloes (i.e. bound substructures which had a progenitor at $z > 10$ with $T_{\rm vir} > 10^4$ K), for the Aq-A-1 (solid line) and the $8\times$ lower resolution Aq-A-2 (dashed line) simulations. Numerical convergence is very good above 100 particles (corresponding to $10^6 h^{-1} M_\odot$ in Aq-A-2). For comparison, the dashed-dotted line is the $z = 0$ mass function of all gravitationally bound substructures in Aq-A-1. *Right panel:* as the left panel, but for the maximum of the circular velocity curve, $V_{\rm max}$.

within the virial radius of the parent halo. To establish the range of descendant masses which are reliably simulated, we begin by carrying out a convergence test of the present-day mass function.

We compare results from the 1.4 billion particle Aq-A-1 simulation with those from the Aq-A-2 simulation which has 8 times poorer resolution. (All six *Aquarius* haloes have been simulated at the resolution of the Aq-A-2 halo; see Table 1). The cumulative mass function of first galaxy haloes that survive to $z = 0$, shown in Fig. 9, shows excellent numerical convergence above a mass of $10^6 h^{-1} M_\odot$, corresponding to 100 particles in Aq-A-2, and to a maximum circular velocity of $V_{\rm max} \sim 5 {\rm km \, s}^{-1}$. We therefore adopt $N_p = 100$ as the resolution limit of the simulations.

Aq-A-2 has 76 surviving first galaxy haloes with $N_p > 100$ ($M > 10^6 h^{-1} M_\odot$). Aq-A-1 has 88 survivors with $N_p > 100$, corresponding to $M > 10^5 h^{-1} M_\odot$ and $V_{\rm max} \sim 2 {\rm km \, s}^{-1}$. Thus, Aq-A-1 resolves dark matter subhaloes with circular velocities lower than the stellar velocity dispersions of the smallest dwarf galaxy satellites of the Milk Way discovered to date (e.g. Simon & Geha 2007).

5.2.1 Abundance of the first galaxies and their descendants

The mass function at $z = 10$ of those 'first galaxy' haloes which ended up inside the virial radius ($\sim 170 h^{-1}{\rm kpc}$ see Table 1) of the main halo today, and the corresponding maximum circular velocity function, are shown in the top two panels of Fig. 10 for all *Aquarius* halos. The most massive of these subhaloes has $M \sim 10^{10} h^{-1} M_\odot$, and circular velocity, $V_{\rm max} \sim 100$ km s^{-1}. There are typically ~ 10 subhaloes with $M > 10^9 h^{-1} M_\odot$ (corresponding to $V_{\rm max} > 40 {\rm km \, s}^{-1}$) and 100 with $M > 10^8 h^{-1} M_\odot$ (corresponding to $V_{\rm max} > 20 {\rm km \, s}^{-1}$).

The lower panels of Fig. 10 give the present day mass and $V_{\rm max}$ distributions of the descendants of the first galaxy halos illustrated in the top panels. Every halo contains ~ 80
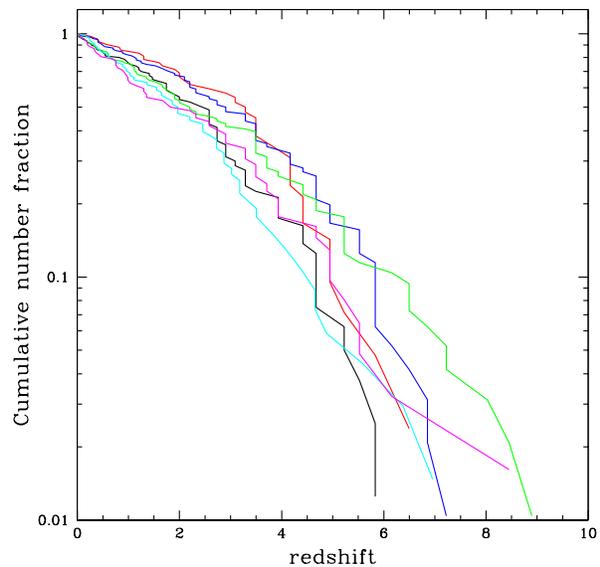
Figure 11. Cumulative fraction of first galaxy haloes that were accreted before a given redshift and survive until $z = 0$. The different lines correspond to the 6 *Aquarius* halos. Typically 50 percent of haloes fell in before $z = 3$.

first galaxy descendants with mass $M > 10^6 h^{-1} M_\odot$ (corresponding to $V_{\rm max} > 5 {\rm km \, s}^{-1}$) that survived since $z = 10$. Note that there is a large variation in the number of survivors in the different *Aquarius* simulations, with the more massive haloes harbouring more massive substructures on average. The mass of the most massive $z = 0$ remnant varies from $3 \times 10^9 h^{-1} M_\odot$ to nearly $10^{11} h^{-1} M_\odot$.

The lower right panel in Fig. 10 shows that, at $z = 0$, the Aq-A-2 halo contains over 60 first galaxy remnant subhaloes
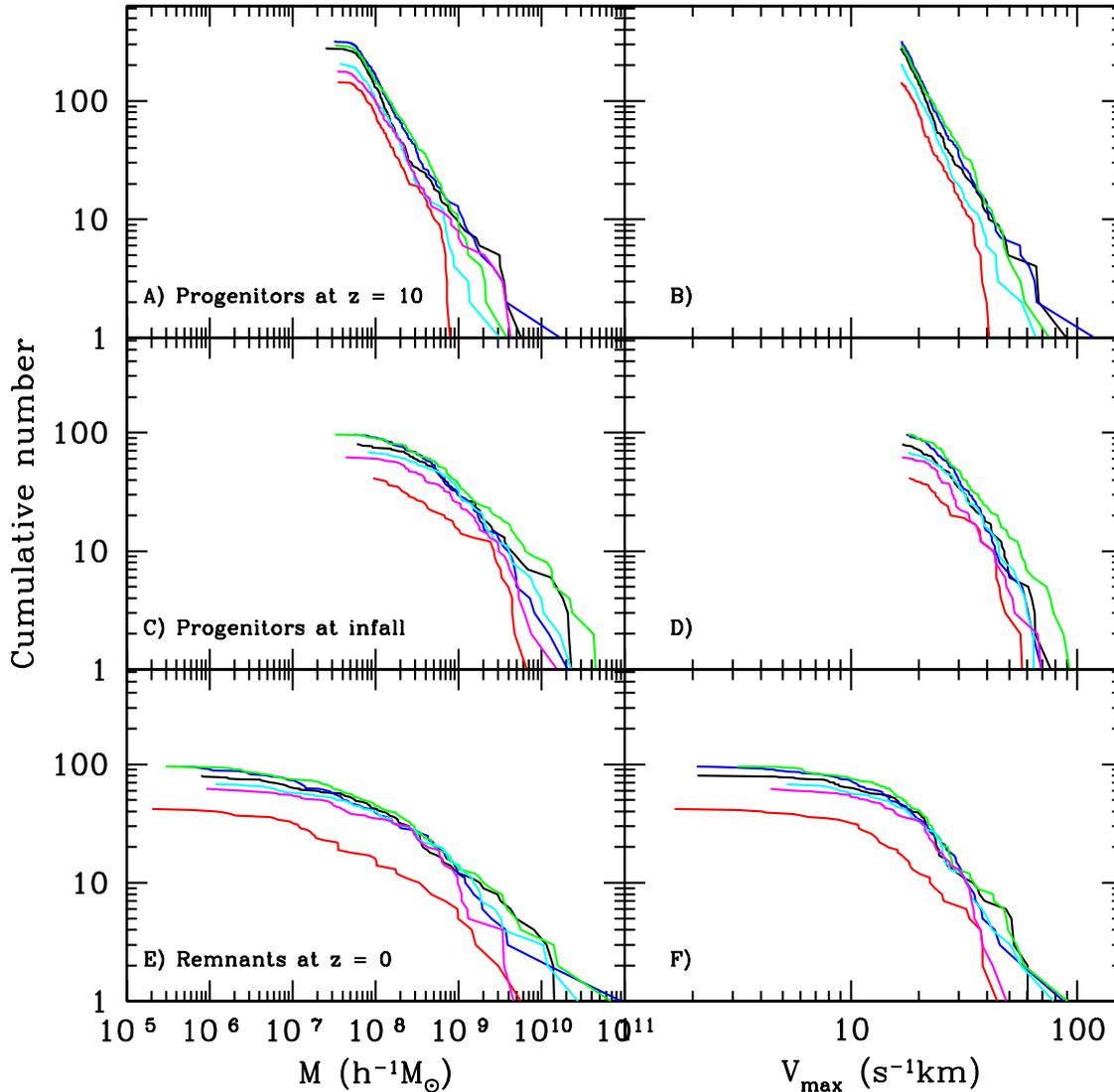
Figure 10. Statistics of first galaxy haloes in all six *Aquarius haloes* (the colour scheme is as in Fig. 1) at z=10 (top), when they are accreted by the main halo (middle), and at $z = 0$ (bottom). The left panels show cumulative mass functions and the right panels show cumulative V_{max} distributions. There is a large variance between the different *Aquarius* haloes at all redshifts. For example, the mass of the most massive $z = 0$ remnant varies between $3 \times 10^9 h^{-1} \mathrm{M}_\odot$ to nearly $10^{11} h^{-1} \mathrm{M}_\odot$. The more massive *Aquarius* haloes tend to have the more massive substructures. Comparing the $z = 0$ masses with those at infall or at $z = 10$ demonstrates that most substructures lose a considerable fraction of their mass by the present.

with $V_{\mathrm{max}} > 10 \mathrm{km\,s}^{-1}$ inside its virial radius. This is a factor of a few larger than the number of classical satellites of the Milky Way. However the *total* (i.e. not just descendants of first galaxies) number of subhalos with $V_{\mathrm{max}} > 10 \mathrm{km\,s}^{-1}$ at $z = 0$ is ~ 400, as may be seen from the right panel of Fig. 9. By contrast, for $V_{\mathrm{max}} > 22 \mathrm{km\,s}^{-1}$ (corresponding to $M \gtrsim 3 \times 10^8 h^{-1} \mathrm{M}_\odot$), the number of *surviving* first galaxy haloes equals the total number of haloes. From SPH simu-

lations of *Aquarius* halos, Okamoto & Frenk (2009) found that *all* subhalos with $V_{\mathrm{max}} = 23.5 \mathrm{km\,s}^{-1}$ host a satellite with V-band luminosity, $L_V > 2.5 \times 10^5 L_\odot$, whereas below that value a diminishing fraction of subhalos manage to make a visible satellite. It is therefore tempting to identify these more massive first galaxy remnants with bright satellite galaxies and to conclude that these must have formed before $z = 10$.

The stellar content of a present day subhalo is thought to be more tightly connected to its dark matter mass at the time when it was first accreted into the main halo than to its current dark matter mass (e.g. Gao et al. 2004a,b. Libeskind et al. 2005). This is because substructures may lose a significant fraction of their dark matter once they have been accreted into the main halo, whereas the more tightly bound stellar content is stripped to a lesser extent. Fig. 11 shows the redshift when first galaxy halos surviving to the present were accreted by the main halo. The median accretion redshift varies between 2 and 3.5 in the different *Aquarius* halos. Less than 1 percent of the halos were accreted before redshift 9 and less than 10 percent before redshift 7. Ninety percent fell in before $z = 1$.

The mass and maximum velocity functions at the time of accretion are shown in the middle panels of Fig. 10. Approximately half of the surviving substructures had a mass, $M > 5 \times 10^8 h^{-1} M_\odot$ ($V_{max} > 30 \mathrm{km\,s}^{-1}$) at infall, compared to their present day values of $M > 1 \times 10^8 h^{-1} M_\odot$ ($V_{max} > 15 \mathrm{km\,s}^{-1}$). Therefore such halos have lost typically 80 per cent of their mass, and their circular velocity has correspondingly decreased by a factor ~ 2.

As discussed earlier, the sites of first galaxy formation are highly clustered and, as a result, feedback may have had an important effect on the number of first galaxies at $z = 10$. However, it is likely that feedback will have not affected the number of first galaxy *remnants* at $z = 0$ since it only influences nearby haloes which are eventually likely to merge. So, although the *stellar properties* of these substructures may have been affected by feedback at $z > 10$, the *number* of remnants is unlikely to depend on the details of this process. As an example, our most extreme feedback model suppresses all star formation within $10 h^{-1}$kpc from a first galaxy, thereby decreasing the number of sites by 30 percent. Yet, the number of first galaxy remnants in this model is the same as that of the no-feedback model.

5.3 Spatial distribution of first galaxy remnants

The remnants of the first galaxies are a small minority amongst surviving subhalos. For example, of the $\sim 10^3$ surviving subhaloes within $R = 20 h^{-1}$kpc in Aq-A-1, only ~ 10 are first galaxy remnants. Their predicted spatial distribution is a useful pointer as to whether observed halo objects could, in fact, be first galaxy remnants.

The top left panel of Fig. 12 shows the cumulative number of first galaxy remnants as a function of distance in both Aq-A-1 and Aq-A-2. Both simulations have about 100 remnants within the virial radius but in the inner part of the halo there are more remnants in Aq-A-1 than in Aq-A-2. The deficit in Aq-A-2 is a resolution effect. As may be seen in Fig. 9, the smallest resolved halos in Aq-A-2 have $V_{max} = 5 \mathrm{km\,s}^{-1}$ whereas in Aq-A-1 they have $V_{max} = 2 \mathrm{km\,s}^{-1}$. These small halos are missing from the central parts of Aq-A-2. Indeed, for $V_{max} > 5 \mathrm{km\,s}^{-1}$, the distributions in the two simulations agree within the errors, as may be seen by comparing the dashed and dotted lines.

The bottom left panel in Fig. 12 shows that the abundance of remnants at a given radius varies by about a factor of 2 between realizations. Five of them have no first galaxy remnants closer to the centre than $10 h^{-1}$kpc, but one of them (Aq-B), has 5, including one at only $3.5 h^{-1}$kpc from

the centre. The top right panel of Fig. 12 shows that the distribution of first galaxy remnants is more centrally concentrated than the overall distribution of *all* surviving subhaloes with $V_{max} > 5 \mathrm{km\,s}^{-1}$. For example, 50% of the first galaxy remnants are within $50 h^{-1}$kpc of the centre, whereas 50% of the subhalo population is within twice that distance. In the outer parts of the halo ($R \gtrsim 40 h^{-1}$kpc), the distribution of first galaxy remnants tracks that of the dark matter but, in the inner parts ($R \lesssim 30 h^{-1}$kpc) it is shallower.

Typically, around 30 first galaxy halo remnants end up in the inner $35 h^{-1}$kpc of the halo. In the Milky Way there are 6 known satellites within this distance which, when allowing for the partial coverage of observational searches for satellites, yields an expected number of ~ 25 dwarfs (Tollerud et al. 2008). The cumulative radial distribution of the 24 known Milky way satellites, normalised to the total number within $120 h^{-1}$kpc, is plotted in the lower right panel of Fig. 12 and is interestingly similar to the distribution of the first galaxy remnants. Detailed treatments of the satellite populations in the *Aquarius* halos may be found in Cooper et al. (2009), Okamoto et al. (2009) and Okamoto & Frenk (2009).

Various physical properties of the first galaxy remnants: mass, V_{max}, half-mass radius, and mean density, ρ, within the half mass radius are plotted in Fig. 13 as a function of distance from the centre in Aq-A-1 and Aq-A-2. The numerical convergence of these properties is very good. As pointed out by Springel et al. (2008), and apparent in the figure, many of the substructures at the two resolutions can be matched spatially. As noted earlier, halos with $V_{max} < 5 \mathrm{km\,s}^{-1}$ are resolved in Aq-A-1, but not in Aq-A-2. This limit approximately corresponds to a mass of $10^6 h^{-1} M_\odot$. Above the resolution limit of Aq-A-2 the results for the two simulations agree remarkably well.

Within $\sim 80 h^{-1}$kpc from the centre, there is a large scatter in the properties of the remnants. Further out, there is a clear increase in mass and V_{max} with radius, reminiscent of the trends found by Springel et al. (2009) for the population of subhalos as a whole. The half-mass radius of the remnants increases systematically with halocentric distance, from about 100 pc in the inner parts to $10 h^{-1}$kpc in the outer parts. The central dark matter densities of the remnants are correspondingly larger in the inner parts. (The apparent convergence of the central density in Aq-A-2 to a constant value at small distances is purely a resolution effect.) The smallest remnants have masses and V_{max} values similar to those of globular clusters.

6 SUMMARY & DISCUSSION

We have used the set of six high resolution cosmological simulations of galactic halos from the *Aquarius Project* (Springel et al. 2009) to investigate the formation and fate of haloes capable of hosting the first stars and the first galaxies. Our main results may be summarized as follows:

First stars

(i) The first halos with virial temperature high enough to form stars, according to the model of Gao et al. (2007), appear at redshift $z = 35$; the number of such haloes in-
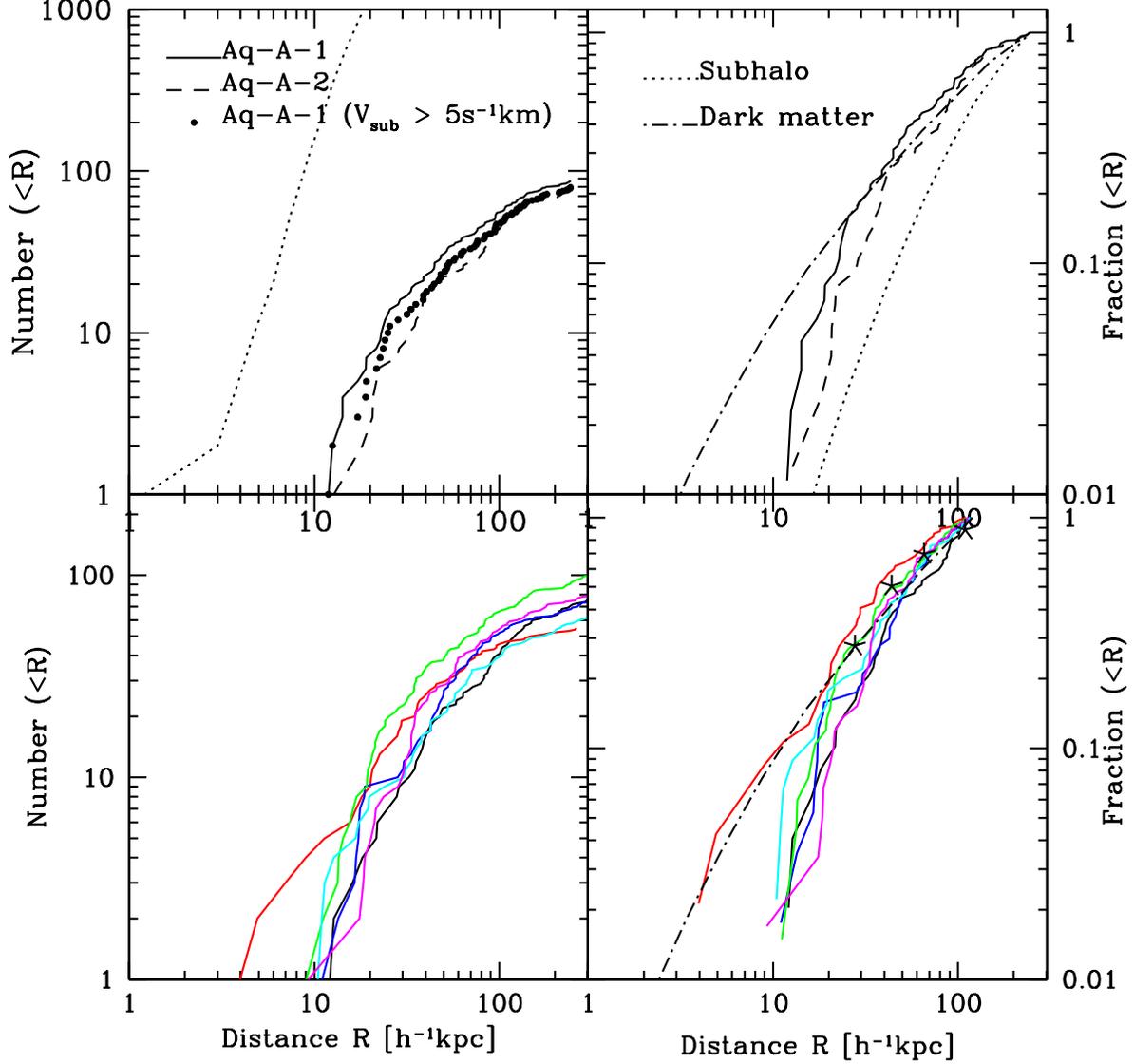
Figure 12. *Left panels*: present day cumulative number of first galaxy halo remnants (i.e. substructures whose progenitors had $T_{vir} >$ 10^4 K at $z = 10$), as a function of distance, R, from the centre of the main halo. In the *top panel*, the solid line shows all halos in Aq-A-1, the thick dotted line halos with $V_{max} > 5 \mathrm{km\,s^{-1}}$ in Aq-A-1 and the dashed lines all halos in Aq-A-2. Halos with $V_{max} < 5 \mathrm{km\,s^{-1}}$ are not resolved in Aq-A-2; for $V_{max} > 5 \mathrm{km\,s^{-1}}$ the distributions in the two simulations agree within the noise. The thin dotted lines shows the cumulative number of *all* substructures with $V_{max} > 2 \mathrm{km\,s^{-1}}$ which is almost two orders of magnitude higher than the number of first galaxy remnants. The *bottom panel* shows results for all 5 level-2 halos. *Top right panel*: as the left panels, but showing the cumulative *fraction* normalised to the number within the virial radius, for Aq-A-1 (thin solid line) and Aq-A-2 (dashed line). *Bottom right panel*: as the left panels, but showing the cumulative *fraction* within $R = 120 h^{-1}$kpc for all 5 *Aquarius* halos. The black solid lines in the top and bottom panels indicate the dark matter profile and the dotted line in the top panel the radial profile of *all* substructures. The pentagons in the lower panel correspond to known Milky Way satellites. Their radial distribution resembles that of the outer first galaxy remnants.

creases exponentially to $\sim 2 \times 10^3$ by $z = 20$ and to $\sim 10^4$ by redshift $z = 10$.

(ii) First star haloes are very highly clustered. The mean interhalo separation increases, in physical units, from $\sim 0.5 h^{-1}$kpc at $z = 25$ to $\sim 1 h^{-1}$kpc by $z = 10$. Thus, if

the HII region created by a Pop. III star is larger than a few hundred parsecs, then feedback due to ionising radiation is likely to have had a large impact on the number of first stars in the proto-galaxy.

(iii) The spatial distribution of the remnants of primor-
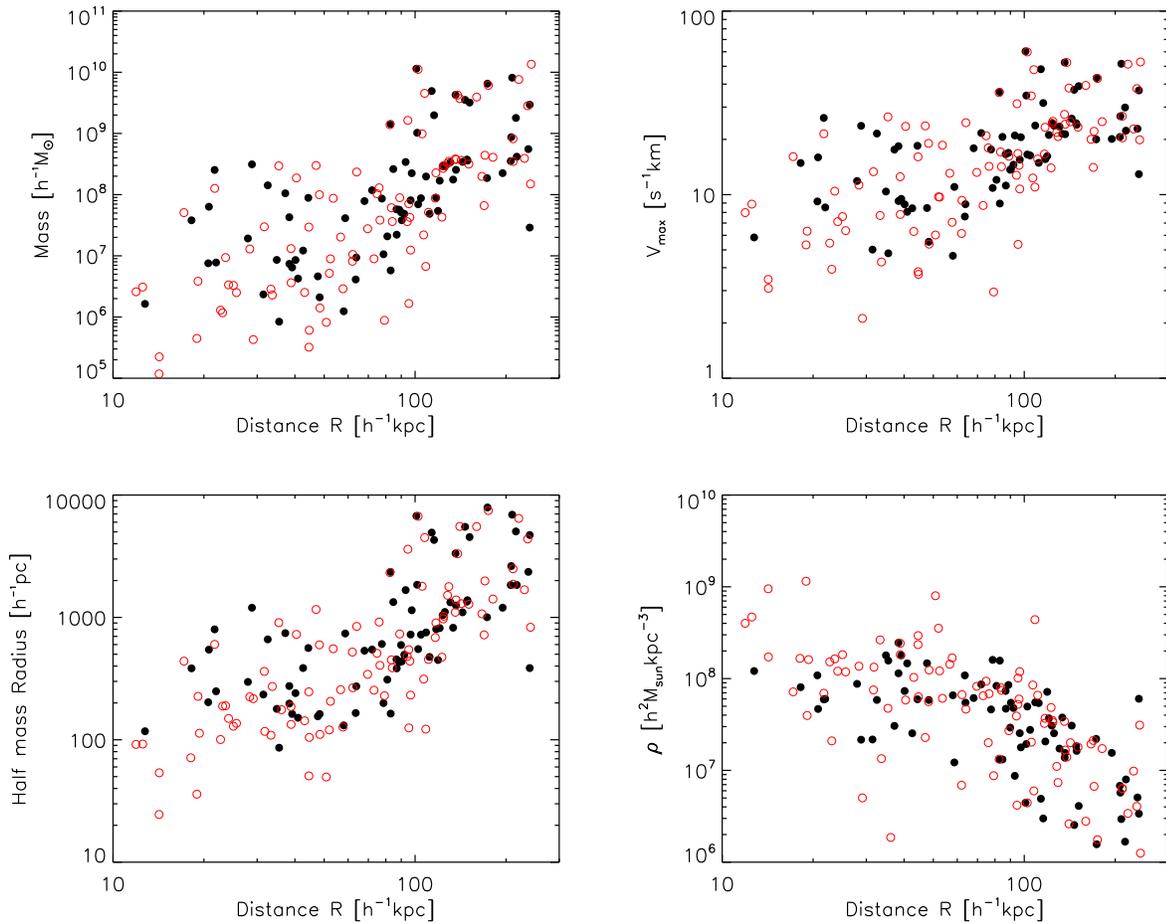
Figure 13. Mass, maximum circular velocity, V_{max}, half-mass radius, and mean density within the half-mass radius, ρ, at $z = 0$ of first galaxy haloes as function of their distance to the centre of the main halo: high resolution simulation Aq-A-1 (*open circles*), and the lower resolution simulation of the same halo, Aq-A-2 (*filled circles*). Resolution effects are noticeable inside $\sim 40h^{-1}$kpc where there are more haloes at higher resolution. More massive haloes tend to be located at $r > 100h^{-1}$kpc. At smaller R there is a large scatter in halo properties, but a notable tendency towards increased subhalo concentration.

dial stars today, as traced by the most strongly bound dark matter particles in the original halo, is more concentrated than that of the dark matter, and scales as $n(R) \sim R^{-2.9}$ with distance, R, from the galactic centre. A few percent of the remnants lie in the galactic bulge, ~ 10 percent in the central $10h^{-1}$kpc of the halo, and ~ 50 percent in the inner $30h^{-1}$kpc of the galactic halo. A significant fraction is associated with subhalos, suggesting that the remnants of some of the first stars could be found today in satellite galaxies, confirming earlier conjectures (e.g. Ricotti & Gnedin 2005; Munoz et al. 2009).

First galaxies

(i) The first pre-galactic halos capable of hosting gas that could undergo atomic hydrogen cooling appear at redshift $z \sim 25$; their number increases to ~ 100 by redshift $z = 20$ and to ~ 300 by at redshift $z = 10$, with substantial scatter from halo to halo. The mean interhalo separation is $4h^{-1}$kpc at redshift $z \sim 20$, and does not evolve much until $z = 10$. Early pre-ionisation by UV photons produced in the first galaxies may have had a significant effect on their numbers

at $z = 10$, although the total number of remnants left over by $z = 0$ is unaffected because most haloes that could plausibly suppress each other's star formation merge by $z = 0$ anyway.

(ii) The majority of the surviving first galaxy halo remnants were accreted into the main halo early. Fifty percent fell in before $z = 3.5$ and ninety percent before $z = 1$.

(iii) About 80 first galaxy halo remnants end up within the virial radius ($\sim 160h^{-1}$kpc) of a galaxy like the Milky Way as satellites with dark matter mass above $10^6 h^{-1} M_{\odot}$ (corresponding to a maximum velocity $V_{\text{max}} \sim 5 \text{km s}^{-1}$). More than half of them had a mass above $5 \times 10^8 h^{-1} M_{\odot}$ ($V_{\text{max}} \sim 20 \text{km s}^{-1}$) before they were accreted by the main progenitor. Many are heavily stripped after infall.

(iv) The spatial distribution of the first galaxy halo remnants today follows that of the dark matter in the outer parts of the galactic halo, but is much less concentrated towards the centre. The remnants, however, are significantly more concentrated than the substructure population as a whole. A typical *Aquarius* halo has 20 first galaxy remnants within $30h^{-1}$kpc of the centre with a velocity dispersion of few kilometers per second, similar to the faintest Milky

Way satellites known. Of course, the presence of the disk may have affected the survival of early substructures.

(v) The mass, V_{max}, and half-mass radius of the first galaxy remnant halos increase with radius. The largest, most massive halos are typically found beyond $100h^{-1}$kpc of the centre. The scatter in these trends increases substantially at smaller radii. At $r < 100h^{-1}$kpc, the median mass of the remnant subhaloes is $\sim 10^7 h^{-1} M_\odot$ and the median V_{max} is ~ 7km s^{-1}.

Our results suggest the following history of early star formation in a galaxy like the Milky Way. Star formation begins at around $z = 35$ in mini-halos and the number of sites where these Pop.III stars can form rapidly builds up to thousands or even tens of thousands depending on the efficiency with which energy from one star prevents neighbouring haloes from making their own star. Since these potential sites are strongly clustered, it is to be expected that many of them will remain barren for some time. A second generation of stars (first star relics) forming near the first stars may be long-lived and their remnants would be found primarily in the inner parts of the galaxy today but also inside satellite galaxies, where they could be identified though their anomalous metallicity patterns.

Following this episode of metal-free star formation, the first 'galaxies' begin to form around $z = 25$. The presence of local radiation sources, enrichment of gas by heavy elements, and possibly mechanical feedback from the first supernovae, may all contribute to a change in the stellar initial mass function, leading to the formation of the first low mass stars. A significant fraction of the haloes that hosted these first galaxies are destroyed by mergers or stripping and their stellar remnants could have contributed to the stellar halo (Cooper et al. 2009). Over 20 percent of the primordial fossils survive as bound structures until the present and some could have developed into satellite galaxies. Our simulations therefore suggest that some of the Milky Way's dwarf satellites should contain a small fraction of the oldest stars that formed during the early stages of formation of the Milky Way.

REFERENCES

Abel T., Bryan G. L., Norman, M. L., 2000, ApJ, 540, 39
Abel T., Bryan G. L., Norman M. L., 2002, Sci, 2002, 295, 93
Abel T., Wise J. H., Bryan G. L., 2007, apjl, 659, L87
Ahn K., Shapiro P. R., 2007, MNRAS, 375, 881
Beers T. C., Christlieb N., 2005, ARA&A, 43, 531
Belokurov, V., et al., 2006, ApJL, 647, L111
Bond J. R., Cole S., Efstathiou G., Kaiser N., 1991, ApJ, 379, 440
Bovill M. S., Ricotti M., 2009, ApJ, 693m 1859
Boylan-Kolchin, M., Springel, V., White, S. D. M., Jenkins, A., & Lemson, G. 2009, MNRAS, 1069
Bromm V., Coppi P. S., Larson R. B., 2002, ApJ, 564, 23
Bromm V., Yoshida N., Hernquist L., 2003, ApJL, 596, L135
Bromm V., Larson R. B., 2004, ARA&A, 42, 79
Bromm V., Yoshida N., Hernquist L., McKee C. F., 2009, Nat, 459, 49
Cole S., Helly J., Frenk C. S., Parkinson H., 2008, MNRAS, 383, 546
Couchman H. M. P., Rees M. J., 1986, MNRAS, 221, 53
Cooper A. et al., 2009, arXiv: 0910.3211
Davis M., Efstathiou G., Frenk C. S., White S. D. M., 1985, ApJ, 292, 371
Diemand J., Madau P., Moore B., 2005, mnras, 364, 367
Efstathiou G., 1992, MNRAS, 256, 43P
Freese K., Bodenheimer P., Gondolo P., Spolyar D., 2009, ApJ, 693, 1563
Gao L., White S. D. M., Jenkins A., Stoehr F., Springel V., 2004a, MNRAS, 355, 819
Gao L., Loeb A., Peebles P. J. E., White S. D. M., Jenkins A., 2004b, ApJ, 614, 17
Gao L., Yoshida N., Abel T., Frenk C. S., Jenkins A., Springel V., 2007, MNRAS, 378, 449
Gao L., Theuns T., 2007, Sci, 317, 1527
Gao L., Navarro, J. F., Cole S., Frenk C. S., White S. D. M., Springel V., Jenkins A., Neto A. F., 2008, MNRAS, 387, 536
Gnedin N. Y., 2000, ApJ, 542, 535
Greif T. H., Johnson J. L., Klessen R. S., Bromm V., 2008, MNRAS, 387, 1021
Haiman, Z., Rees, M. J., & Loeb, A. 1996, ApJ, 467, 522
Haiman Z., Rees M. J., Loeb A., 1997, ApJ, 476, 458
Heger A., Fryer C. L., Woosley S. E., Langer N., Hartmann D. H., 2003, ApJ, 591, 288
Helmi A. et al., 2006, ApJL, 651, L121
Hoeft M., Yepes G., Gottlöber S., Springel V., 2006, MNRAS, 371, 401
Iwamoto N., Umeda H., Tominaga N., Nomoto K., Maeda K. 2005, Science, 309, 451
Kirby E. N., Simon J. D., Geha M., Guhathakurta P., Frebel A., 2008, ApJL, 685, L43
Komatsu E., et al. 2009, ApJS, 180, 330
Koposov S. E., Yoo J., Rix H.-W., Weinberg D. H., Macciò A. V., Escudé, J. M., 2009, ApJ, 696, 2179
Krumholz M. R., McKee C. F., 2005, ApJ, 630, 250
Lacey C., Cole S., 1993, MNRAS, 262, 627
Libeskind N. I., Frenk C. S., Cole S., Helly J. C., Jenkins A., Navarro J. F., Power C., 2005, MNRAS, 363, 146
Machacek M. E., Bryan G. L., Abel T., 2003, MNRAS, 338, 273
Madau P., Diemand J., Kuhlen M., 2008, ApJ, 679, 1260
McKee C. F., Tan J. C., 2008, ApJ, 681, 771
Munoz J. A., Madau P., Loeb A., Diemand J., 2009, MNRAS, 400, 1593 arXiv: 0905.4744
Mori M., Ferrara A., Madau P., 2002, ApJ, 571, 40

Navarro J. F., et al., 2008, arXiv:0810.1522

Okamoto T., Gao L., Theuns T., 2008, MNRAS, 390, 920

Okamoto T., et al. 2009, MNRAS, 399, 174L

Okamoto T., Frenk C. S., Jenkins A., Theuns T., 2009, MNRAS, arXiv:0909.0265

O'Shea B. W., Norman M. L. 2007, ApJ, 654, 66

O'Shea B. W., Norman M. L. 2008, ApJ, 673, 14

O'Shea B. W., McKee C. F., Heger A., & Abel T., Xarchiv:0801.2124

Press W. H., Schechter P., 1974, ApJ, 187, 425

Reed D. S., Bower R., Frenk C. S., Gao L., Jenkins A., Theuns T., White S. D. M., 2005, MNRAS, 363, 393

Ricotti M., Gnedin N. Y., 2005, ApJ, 629, 259

Rollinde E., Vangioni E., Maurin D., Olive K. A., Daigne F., Vincent F., 2008, arXiv:0806.2663

Rollinde E., Vangioni, E., Maurin, D., Olive, K. A., Daigne, F., Silk, J., Vincent, F. H. 2009, MNRAS, 398, 1782

Schaerer D. 2002, A&A, 382, 28

Schneider R., Omukai K., Inoue A. K., Ferrara A., 2006, MNRAS, 369, 1437

Shapiro P. R., Iliev I. T., Raga A. C., 2004, MNRAS, 348, 753

Simon J. D., Geha M., 2007, ApJ, 670, 313

Springel, V., White, S. D. M., Tormen, G., & Kauffmann, G. 2001, MNRAS, 328, 726

Springel V., 2005, MNRAS, 364, 1105

Springel V. et al., 2005,Nat, 435, 639

Springel V., et al., 2008a, Nat, 456, 73

Springel V., et al., 2008b, MNRAS, 391, 1685

Sokasian A., Yoshida N., Abel T., Hernquist L., Springel V. 2004, MNRAS, 350, 47

Tegmark M., Silk, J., Rees M. J., Blanchard A., Abel T., & Palla F. 1997, ApJ, 474, 1

Thoul A. A., Weinberg D. H., 1996, ApJ, 465, 60

Tollerud E. J., Bullock J. S., Strigari L. E., Willman B., 2008, ApJ, 688, 277

Willman B., et al., 2005, ApJL, 626, L85

Whalen D., Norman M. L., 2008a, ApJ, 673, 664

Whalen D., O'Shea B. W., Smidt J., Norman M. L., 2008b, ApJ, 679, 925

White, S. D. M., & Frenk, C. S. 1991, ApJ, 379, 52

White S. D. M., Rees M. J. 1978, MNRAS, 183, 341

White S. D. M., & Springel, V., 2000, The First Stars. Springer-Verlag, Berlin P. 237

Wise J. H., Abel T., 2008, ApJ, 685, 40

Yoshida N., Abel T., Hernquist L., Sugiyama N., 2003, ApJ, 592, 645

Yoshida N., Omukai K., Hernquist L., Abel T., 2006, ApJ, 652, 6

Yoshida N., Oh S. P., Kitayama T., Hernquist L., 2007, ApJ, 663, 687